Nanostructured functionalised niobium oxide as chemoselective catalyst for acetalation of glucose

Sahil Kumar[123], Kanika Saini[1], Shunmugavel Saravanamurugan*[1] Xiaolei Zhang*[2] and Sushil Kumar Kansal*[4]

[1]*Laboratory of bio-product chemistry, Center of Innovative and Applied Bioprocessing, Mohali- 140 306, Punjab, India*

[2]*Department of Chemical and Process Engineering, University of Strathclyde, United Kingdom*[3]*Energy Research Centre, Panjab University, Chandigarh.*

[4]*Dr. S. S. Bhatnagar University Institute of Chemical Engineering and Technology, Panjab University, Chandigarh- 160 014, India*

ORCID: SK: 0000-0003-2935-5932, KS: 0000-0003-4809-730X, SS: 0000-0002-3980-5020, XZ: 0000-0001-9415-3136, SKK:0000-0001-7480-7227.

Corresponding authors- saravana@ciab.res.in, sushilkk1@pu.ac.in, xiaolei.zhang@strath.ac.uk

Abstract

Developing a chemoselective catalyst for the acetalation of biomass-derived glucose to alkyl glycosides has been recognised as an emerging field due to its wide range of applications. The present study focuses on synthesising sulfate functionalised niobium oxide-based (NbOx-DS) catalyst to introduce medium/strong acidic sites that contribute to the catalytic activity towards glucose acetalation, which has not been explored previously. The nanosized NbOx-D is prepared via a precipitation approach using niobium chloride and diethylamine as a precursor and precipitating agent, respectively. The sulfate groups incorporated NbOx-DS gives a good yield of ethyl glucosides (60%) with excellent selectivity (97%) in ethanol. On the other hand, the sulfate groups incorporated into the commercial niobium oxide (NbOx-CS) exhibits poor catalytic activity, yielding 6% ethyl glucoside with a low selectivity (8%). FTIR analysis corroborates the incorporation of sulfate groups in the NbOx-DS matrix, unlike NbOx-CS. XRD pattern of NbOx-DS shows a lower angle shift of a peak to 23.5° compared to parent NbOx-D (24.32°), indicating lattice expansion due to the incorporation of sulfate groups, and no such a shift in the case of NbOx-CS is observed. NH_3-temperature programmed desorption (NH_3-TPD) reveals that NbOx-DS possess a 2.1-fold higher number of acidic sites than NbOx-D, whereas NbOx-CS possess a negligible number of acidic sites, indicating the significance of the synthesis procedure of

This is a peer-reviewed, accepted author manuscript of the following article: Kumar, S., Saini, K., Saravanamurugan, S., Zhang, X., & Kansal, S. K. (2022). Nanostructured functionalised niobium oxide as chemoselective catalyst for acetalation of glucose. Topics in Catalysis. https://doi.org/10.1007/s11244-022-01738-8

NbOx-D for efficient incorporation of sulfate groups. NbOx-DS displays recyclability for at least three runs with minor loss in the activity. In a nutshell, the current study reflects that NbOx-DS obtained via precipitation followed by sulfate groups incorporation increases the medium/strong acidic sites, which contributes significantly to enhancing the ethyl glucoside selectivity (97%).

Keywords: Acetalation, niobium oxide, sulfate groups, glucose, ethyl glucosides

Graphical abstract

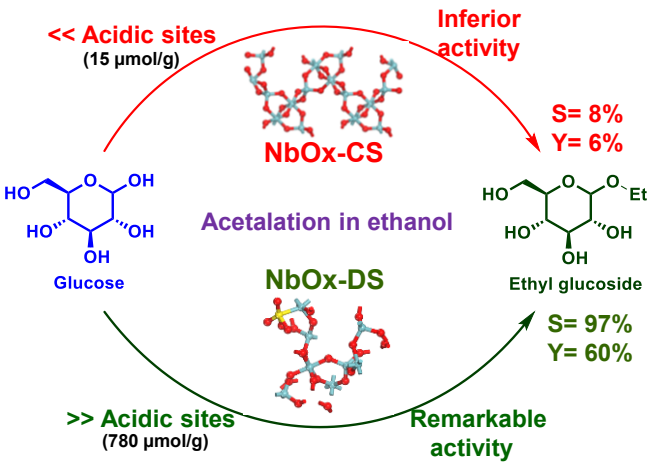

1. Introduction

The 21st century is witnessing a continuous increase in the demand for chemicals and fuels due to the increasing global population. The exponential growth in the industrial sector is constantly dwindling as it predominantly relies on non-renewable fossil resources, thus necessitating the search for more sustainable alternatives. In this regard, terrestrial lignocellulosic biomass is an indispensable, sustainable carbon-rich source that has the potential to substitute fossil feedstocks for the production of a diverse range of fine chemicals [1-3]. Mainly, cellulose is the major component (> 50%) of most lignocellulosic biomass than hemicellulose and lignin, composed of glucose units connected with β-1,4 linkages, thus making glucose a potential substrate for the

production of value-added products. However, the effective utilisation of glucose is challenging for chemical industries due to the formation of undesired byproducts or humins during the process, which not only reduces the process efficiency but also inhibits the catalytic reactions by the deactivation of active sites. [4-5].

As mentioned above, glucose can be used as a starting substrate to produce a wide range of chemicals, such as 5-hydroxymethyl furfural (5-HMF), glucaric acid, lactic acid, levulinic acid, and alkyl glucosides (AGs) via dehydration, oxidation, hydrogenation, and acetalation, respectively [6-11]. Among all these reactions, acetalation is a well-known biological, chemical and pharmaceutical process. The acid-catalysed acetalation of glucose with alcohols is considered a crucial reaction in many industries, such as Integrated chemicals specialities, Nouryon, WanQi, Libracare, Norfox, IRO coating additive Co., Ltd and BASF, for the synthesis of AGs [12-16]. AGs are known for nonionic bio-based surfactants with huge applications in pharmaceuticals, cosmetics, emulsifiers, and cleaning processes [17]. AGs, such as Libracare APG06, a hexyl glucoside-based surfactant, is highly stable in basic media and thus suitable for industrial cleaning agent [18]. The market size of AGs is anticipated to reach USD 911 million and is further expected to grow with a compound annual growth rate (CAGR) of 5.6% by 2026 [19]. Despite their large market size, AGs are relatively expensive compared to surfactants derived from non-renewable resources having similar properties [20-21]. This indicates the requirement for the upgradation of the process with robust catalytic systems. Currently, AGs are produced by using sulfuric acid as the sole catalyst with glucose as starting substrate, affording a 70% yield of alkyl polyglycosides [21, 22-24]. However, this process entails neutralising the effluent using the basic solution of sodium hydroxide, leading to the formation of salt (Na_2SO_4), which is undesirable. In addition, the process exhibits environmental hazards, corrosion to the reaction vessel, relatively lower yield, undesired product formation, and non-separation of salt from the reaction mixture. To overcome these issues, heterogenous catalysts containing a large number of acidic sites are required to replace traditional homogeneous acid catalysts [25].

Solid acid catalysts are pivotal in catalysis, offering easier separation, recyclability and higher thermal stability [26-27]. In this regard, solid acid catalysts such as sulfate acid–silica gel (H_2SO_4/SiO_2), Amberlyst-15, Nafion SAC-13, SO_3H-SBA-15 and $H_3PW_{12}O_{40}$ have been reported for the production of AGs, giving moderate to good yields of AGs (40-80%) [28-31]. However, these catalytic systems produce many unwanted byproducts, possibly deactivating the active catalytic sites, thus limiting their activity and viability compared to homogenous acids. To overcome the abovementioned disadvantages, functionalised polymeric materials have been

developed, such as polystyrene-supported sulfonic acid and polyvinyl trisulfonate ethylamine-based catalysts for the acetalation reactions [32-33]. However, the highly tedious synthesis procedure, entailing malignant toxic/hazardous chemicals such as triethanolamine, chloroethanol, and chlorosulfonic acid with bulky organic functional groups, limits its industrial applicability. In line with this, over the past few years, water-tolerant solid acid-based catalysts, such as Nb_2O_5 and ZrO_2, have been investigated due to their high thermal stability and tuneable acidic properties [9, 34-35]. Usually, while performing catalytic experiments in aqueous media, several solid acid catalysts lose their activity because of active site poisoning via the formation of lewis acid-base adduct, thus not industrially viable. For example, in an aqueous medium, sulphated zirconia and zeolite-based catalysts exhibited a significant decline in the catalytic activity towards hexane isomerisation and phenyloxirane hydrolysis reactions, reflecting acidic site deactivation by water [36,37].

Interestingly, being a water-tolerant solid acid catalyst, NbOx showed enhanced activity in the hydrolysis of phenyloxirane than zeolite [36] and in glucose dehydration to 5-HMF. Therefore, developing water-tolerant acidic niobium oxide is an exciting approach for the acetalation reactions as water forms as a byproduct. Various niobium oxide-based catalysts, such as ternary nanocomposites (Nb_2O_5RGO/MoO_3), Nb_2O_5 grafted on glass foams, niobium carbides, and niobium oxyhydroxide, have also been widely studied for different reactions, including photocatalytic applications, dye degradation for removal of water pollutants and carbon dioxide conversion to fuels and chemicals; thus, implying the broad range applicability of niobium oxide as a potential catalyst or as a support in catalytic industries [38-41]. The robust nature of Nb_2O_5 has stimulated researchers worldwide for its catalytic application, but lacking in medium/strong Bronsted acidic sites, which are required for various reactions, such as dehydration, acetalation, and trans-esterification reactions [42-44]. Incorporating the sulfate groups in the NbOx matrix is an effective strategy for enhancing the Bronsted acidity, which has a similar strength to sulfuric acid-based catalysts and has received much attention recently due to its versatile applications in the chemical industries. The major issues with the reported NbOx-based catalytic system are the formation of humins and lower thermal stability, consequently reducing selectivity towards the desired product and thus deactivating the active sites on the catalyst surface [45-49].

Here, we report the synthesis of sulphate groups incorporated Nb_2O_5 and their characterisation with various techniques, such as XRD, FTIR, NH_3-TPD, BET, HR-TEM and TGA. The characterised material is examined for the acetalation of glucose in ethanol to obtain ethyl glucosides. The catalytic activity of Nb_2O_5

before and after incorporating sulfate groups is also studied to emphasise the role of medium/strong Bronsted acid sites towards acetalated products.

2. Experimental

2.1. Materials

Niobium chloride, diethylamine, sulphuric acid, D-glucose, and niobium oxide were bought from Sigma-Aldrich. Absolute ethanol (99.8%) was purchased from Fischer scientific chemicals. Ethyl-α-glucopyranoside and ethyl-β-glucopyranoside were purchased from Biosynth carbosynth. All the chemicals were directly used as received.

2.2. Catalyst preparation

Niobium oxide was first prepared using niobium chloride as a metal precursor and diethyl amine as a precipitant, followed by hydrothermal treatment. In a typical procedure, 0.4 mol of niobium chloride was dissolved in an appropriate amount of water, and then 2.0 mol of diethylamine was added dropwise. Afterwards, the solution was transferred to Teflon lined autoclave and sealed properly with the help of a torque wrench to avoid pressure leakage and kept in the oven at 140 °C for 20 h. The mixture was then allowed to cool down overnight. The formed white precipitate was filtered off, washed with a water-methanol mixture to neutral pH, and dried in the hot-air oven at 80 °C. The dried powder was ground well with a mortar and pestle and transferred to a quartz crucible for calcination under static air at 400 °C for 4 h at a ramp rate of 2 °C/min, and the final product was designated as NbOx-D.

An appropriate amount of niobium oxide was refluxed in the diluted aqueous sulfuric acid at 80 °C for 3 h. The slurry was then filtered off, washed with plenty of water and dried in the oven at 80 °C overnight. The obtained powder was designated as NbOx-DS. Similarly, NbOx-CS was prepared under similar conditions using commercial niobium oxide for comparison.

2.3. Catalytic reactions

The catalytic acetalation of glucose was carried out in a 15 ml ace pressure tube. 0.126 mmol of glucose, 2 ml of ethanol and 20 mg of catalyst were placed in an ace pressure tube and closed tightly. The pressure tube was placed in a preheated silicon oil bath on a hot plate with a magnetic stirrer and ran at the required temperature and time. After each experiment, the pressure tube was cooled down to below room

temperature using ice-cold water. A fraction of each reaction mixture was taken out and filtered off using a 0.2 µm syringe filter before HPLC analysis (Thermofisher ultimate 3000; column: Aminex HPX-87H, 60 °C; Eluent: 5mM sulfuric acid). The glucose conversion and product yield (ethyl α-D-glucopyranoside, ethyl β-D-glucopyranoside) were calculated using a series of individual standards by standard calibration.

2.4. Characterisation

X-ray diffractometer (XRD) technique (Bruker D8 discover; Cu-K alpha radiation, λ= 1.5406 A°, 40 kV, 40 mA) is used to understand and identify the crystallinity and crystal phase of the material. The XRD patterns were collected in the 2θ range of 5-70° with a step size of 0.020° per second, and total steps recorded were 3221 with an estimated time per step was 192 seconds.

NH_3-temperature-programmed desorption (NH_3-TPD) is a chemisorption technique used for acidic site determination using a BELCAT II instrument equipped with a thermal conductivity detector (TCD). The typical procedure follows: 50 mg of catalyst was loaded in a quartz tube and pretreated at 80 °C for 60 min under a 50 ml/min flow of helium gas to remove the physisorbed water molecules. The adsorption of ammonia was performed using a 5.1% NH_3/He mixture with a flow of 50 ml/min for 30 min at 50 °C, followed by flushing with 50 ml/min He to remove physisorbed ammonia. Finally, ammonia desorption was performed from 50 to 500 °C at a ramp of 10 °C/min.

Thermogravimetric analysis (TGA) (NETZSCH; coupled with differential scanning calorimetry; 50 ml N_2/min) reveals the thermal stability and weight loss of the material. The TGA thermograph was obtained between 25 and 550 °C with a hold time of 20 min.

Fourier transform Infrared (FTIR) (Horizon MB 3000) spectroscopy technique is used to disclose the nature of the functional groups present in the material. The FTIR spectra were measured in the range of 400-4000 cm^{-1}.

Physisorption analysis (ASAP 2420) is employed to quantify the surface area, pore volume and pore size of the material using N_2 as a probe molecule. Prior to analysis, all the samples were degassed at 150 ºC for 4 h under vacuum.

Microscopic techniques (high-resolution transmission electron microscope (HRTEM); JEOL 2100 Plus; 200 KV) are beneficial in visualising the particle size of the material in addition to observing morphology

and lattice fringes. HRTEM coupled with Energy Dispersive X-ray (EDX) is used to disclose the elemental composition of the material. For sample preparation, a small amount of the sample was dissolved in ethanol, followed by sonication for 30 min, and then the sample was carefully dropped on a copper grid with the help of a micropipette, dried in the air, and employed for analysis.

3. Results and Discussion

Niobium oxide with and without sulfate functional groups were examined for the acetalation of glucose in ethanol as solvent at 120 °C, and the results are presented in Table 1. Generally, the acetalation of glucose in alcohol (ethanol) leads to the formation of two tautomers, that is, ethyl α-D-glucopyranoside (EADGP) and ethyl β-D-glucopyranoside (EBDGP) (Scheme 1) in the presence of Bronsted-acidic sites on the catalyst surface. The plausible reaction pathway for the formation of ethyl glucoside from glucose in ethanol can take place in three steps [5] as follows; 1) ring opening of glucose in the presence of an acid catalyst, 2) the hemiacetal formation by reaction between the aldehyde group of glucose and ethanol, followed by 3) the removal of a water molecule to form cyclic acetal, ethyl glucoside. Initially, the niobium oxide prepared using niobium chloride as precursor and diethylamine as precipitant (NbOx-D) was tested for glucose acetalation and found to be affording only EADGP with a low yield (13%) at a glucose conversion of 79.8% (Table 1, entry 1) with the formation of fructose, HMF and humins as byproducts.

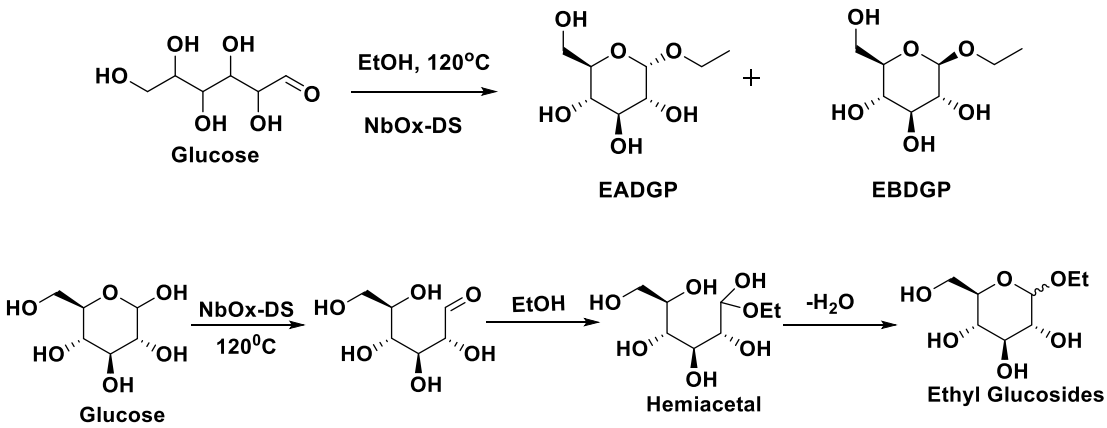

Scheme 1. Acetalation of glucose in ethanol (above) and the plausible reaction pathway for the formation of ethyl glucosides

On the other hand, sulfate incorporated NbOx-D (treated with sulfuric acid, i.e. NbOx-DS) exhibited a higher catalytic activity, affording a total yield of 59.9% (36.3% EADGP and 23.6% EBDGP) with a selectivity of 97%, implying the role of medium/strong acid sites generated by the incorporated sulfate groups (Table 1, entry 2). The sulfate groups incorporated on commercial niobium oxide (NbOx-CS) was also investigated under similar reaction conditions and gave a relatively low yield of total ethyl glucosides (5.6%) with a poor selectivity of 8.1 %. To understand the catalytic activity discrepancy, structural and physicochemical properties of niobium oxide with and without sulfate groups were evaluated using typical characterisation techniques.

Table 1. Screening of sulfate functionalised NbOx catalysts for glucose acetalation

Entry	Catalyst	Glucose Conv. (%)	EBDGP yield (%) *	EADGP yield (%) **	Selectivity (%)
1	NbOx-D	79.8	13.2	---	16.5
2	NbOx-DS	62.0	36.3	23.6	96.6
3	NbOx-CS	68.7	-----	5.6	8.15

Reaction conditions: 0.126 mmol of glucose, 20 mg catalyst, 2 ml ethanol, 120 °C, 2 h.

3.1. XRD analysis

The X-ray diffraction pattern of NbOx-D showed two major peaks at 2θ of 24.35 and 26.85° along with low-intensity peaks at 46.6 and 55.1, ascribing to the orthorhombic phase of niobium oxide [JCPDS-30-0873]. NbOx-DS displayed drastic crystallinity loss and showed a slight shift towards a low angle at 2θ of 23.5 from 24.35° (Figure 1a), indicating the lattice expansion due to the incorporation of bulky sulphate groups in the network of niobium oxide [50, 51]. On the other hand, NbOx-CS showed no shift in 2θ position of peaks (Figure 1b) and thus, suggesting incompetent incorporation of sulphate groups in the commercial niobium oxide matrix and, therefore, showing inferior catalytic activity compared to NbOx-DS [Table 1, entry 2 and 3]. The lower angle shift in the case of NbOx-DS compared to NbOx-D indicated the incorporation of active sulfate functional groups, which played a crucial role in enhancing the yield of ethyl glucosides and its selectivity (96.6%) [Table 1, entry 2]. However, XRD does not provide direct evidence for incorporating sulphate species; the samples were further analysed using FTIR.

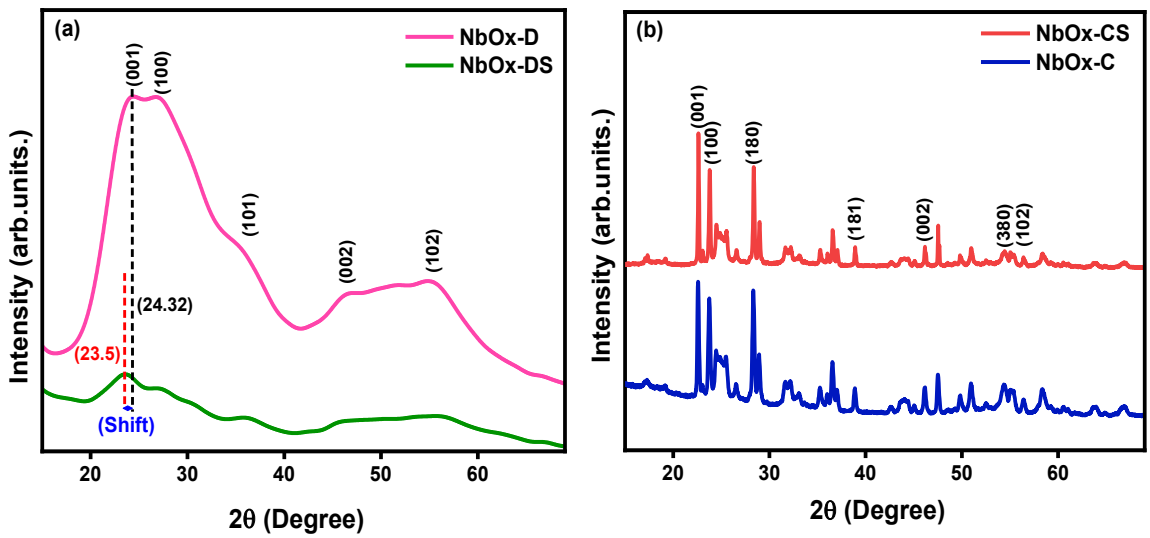

Figure 1. X-ray diffraction pattern of (a) NbOx-D and NbOx-DS and (b) NbOx-C and NbOx-CS catalysts

3.2. FTIR analysis

The presence of the sulfate functional groups was substantiated by subjecting the samples to Fourier transform infrared analysis (FT-IR) (Figure 2). Generally, the sulphate group exists in tetrahedral symmetry (T_d). But NbOx-DS displays three peaks at wavenumbers of 1047, 1141 and 1203 cm^{-1} corresponding to S=O stretching frequencies, suggesting lowered symmetry of SO_4^{2-} from tetrahedral geometry to $C_{2v,}$ which could be due to the coordination of disulfate species with niobium [52-53]. And no such peaks appeared in the case of non-functionalised NbOx-D catalyst. Additionally, both NbOx-D and NbOx-DS exhibit bands at 1620 cm^{-1} due to the bending mode of water molecules in niobium oxide [52]. Moreover, broad bands appearing in the 2800-3600 cm^{-1} can be ascribed to stretching modes of -OH groups in niobium oxide. Moreover, in the case of the NbOx-DS catalyst, it can be noticed that the intensity of the broad band in the region of 2800-3600 cm^{-1} slightly decreased compared to the band in NbOx-D due to the incorporation of sulfate moiety in the terminal position of niobium oxide by reacting with -OH groups [53-54]. In the case of NbOx-CS and NbOx-C, no such band appeared in the region of 800-4000 cm^{-1}, suggesting the scarcity of easily accessible hydroxyl groups that can react with sulfate species in commercial niobium oxide, thus showing poor/negligible incorporation and consequently displaying insignificant catalytic activity [Table 1, entry 3].

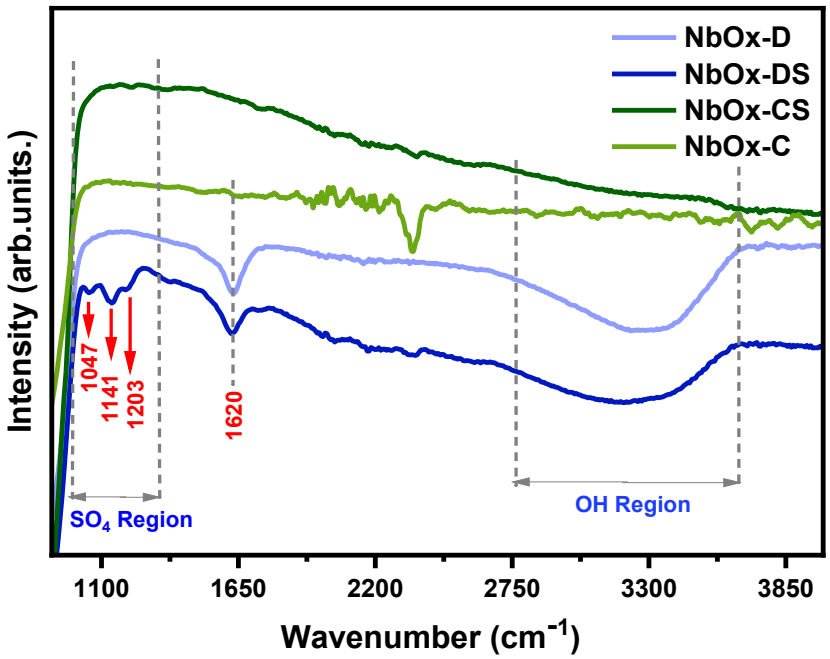

Figure 2. Fourier transform infrared spectra of NbOx catalysts

3.3. Structural analysis

To estimate the particle size and changes in the nanostructure before and after the sulfate incorporation, NbOx-D and NbOx-DS were characterised with HR-TEM (Figures 3 and 4). The particle size of NbOx-D was around 10 nm (Figure 3a), calculated through ImageJ software (Figure 3d). Figure 3b shows the lattice fringes with a d-spacing of 0.385 nm, corresponding to the (001) planes with a symmetrical arrangement of the lattice plane (Figure 3b inset). The EDX spectrum indicates that NbOx-D possesses niobium and oxygen with no other chemical impurities (Figure 3c). On the other hand, NbOx-DS showed a similar particle size of around 10 nm (Figure 4h). A high-resolution image of NbOx-DS exhibited lattice fringes corresponding to (001) planes with a slight lattice distortion with an increased d-spacing of 0.395 nm (Figure 4f inset). The rationale behind this imperfection in lattice fringes might have been caused by the incorporation of sulfate groups in the matrix of niobium oxide as in line with XRD (Figure 1). The EDX spectrum of NbOx-DS evidently displays the presence of sulfur, niobium, and oxygen species (Figure 4g).

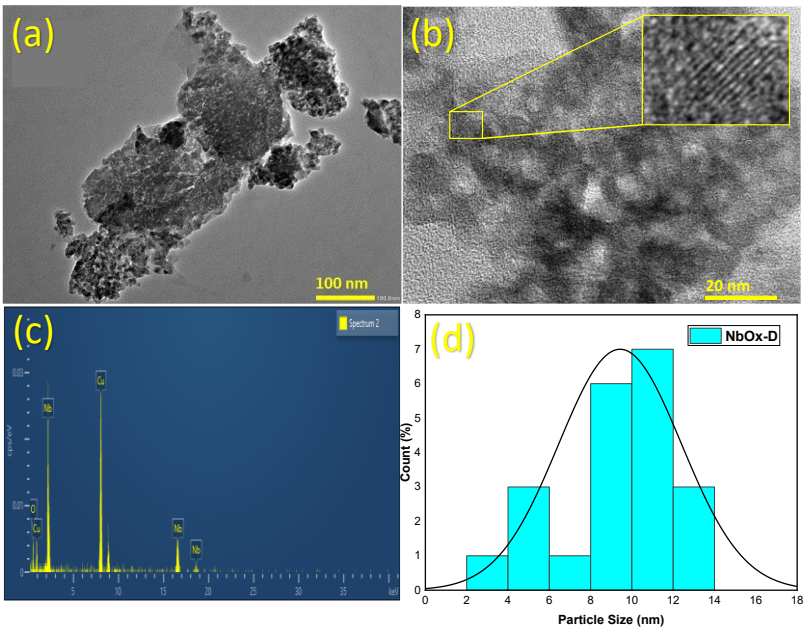

Figure 3. HR-TEM images of NbOx-D with low (a) and high (b) resolution, EDX Spectrum (c) and particle size distribution (d).

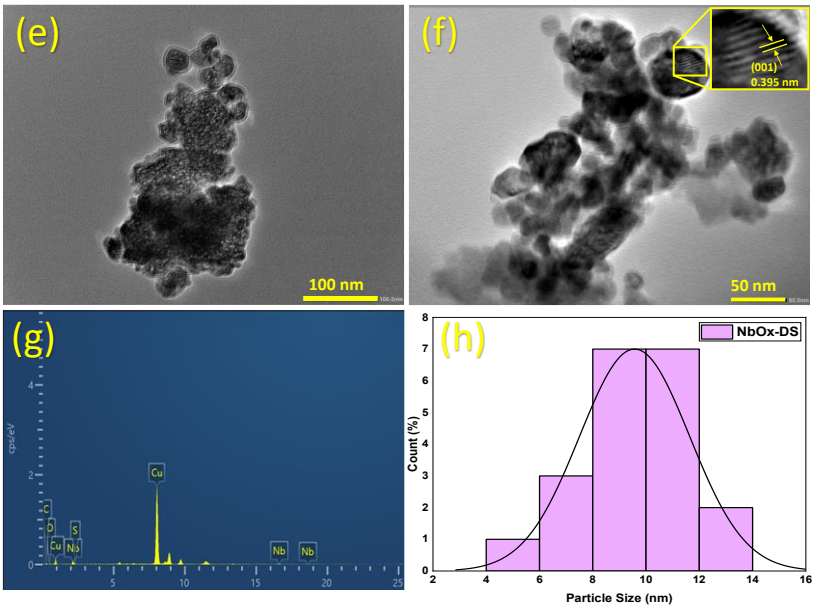

Figure 4. HR-TEM images of NbOx-DS with low (a) and high (b) resolution, EDX Spectrum (c) and particle size distribution (d).

3.4. Ammonia TPD analysis

It is known that the formation of ethyl glucosides from glucose proceeds via acetalation, which mainly depends on the strength of acidic sites present over a catalyst surface [55]. To understand the nature of the acidic

sites, all the niobium oxide-based catalysts were subjected to NH_3-TPD, and the corresponding profiles are shown in Figure 5. NbOx-DS contained total acidic sites of 783 µmol/g, whereas NbOx-D possessed relatively lower (628 µmol/g), which is 1.25-fold lower than the former, indicating the incorporation of sulfate species contributing to the acidic sites. NbOx-C and NbOx-CS exhibited negligible acidic sites of 5 and 15 µmol/g, respectively. The NH_3-TPD profiles of NbOx-D and NbOx-DS appeared unsymmetrical in peak pattern and thus deconvoluted (Figures 5b and 5c). The deconvoluted peaks are categorised as Type I (weak; 50-180 °C), Type II and III (medium; 180-350 °C) and Type IV (strong; 350-500 °C), as reported in the previous study [9, 56]. NbOx-DS possessed 2.1-fold higher type II and III acidic sites than NbOx-D (317 µmol/g). However, NbOx-D had 2.9-fold higher type I acidic sites than NbOx-DS catalyst, which might be contributing to catalysing glucose isomerisation rather than acetalation, thus, decreasing the yield of ethyl glucopyranosides [Table 1, entry 1]. Further, NbOx-DS (736 µmol/g) possessed 1.5-fold higher medium and strong acidic sites than NbOx-D (490 µmol/g). Moreover, NbOx-DS displayed an intense desorption peak (medium acidic sites) around 210 °C, having 1.9-fold higher than NbOx-D (229.8 µmol/g).

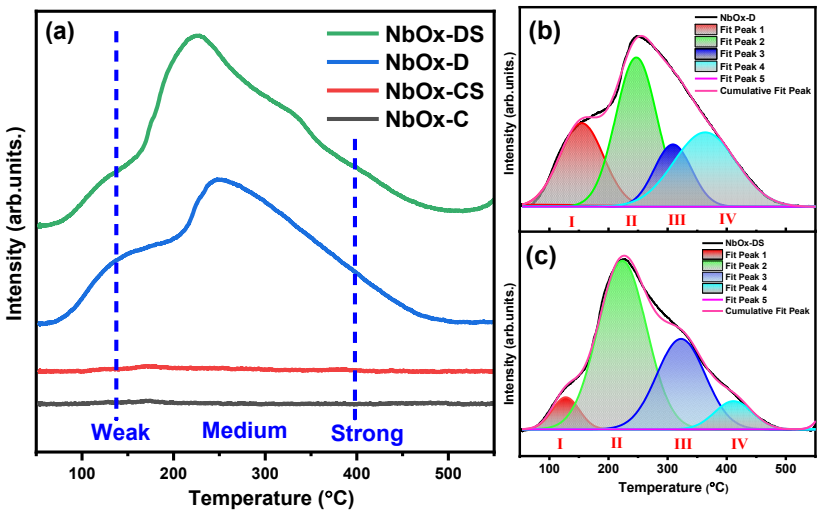

Figure 5. NH_3-TPD profile of a) NbOx catalysts and deconvoluted b) NbOx-D and c) NbOx-DS.

From the above viewpoints, it can be concluded that possessing a large number of acidic sites with higher strength (NbOx-DS) played a pivotal role in enhancing the total yield of ethyl glucosides with excellent selectivity (yield:60%; selectivity: 97%) [Table 1, entry 2]. At the same time, NbOx-D possessed relatively lower number of medium/strong acid sites, yielding poor selectivity towards ethyl glucosides (yield:13%; selectivity: 17%) [Table 1, entry 1]. Based on NH_3-TPD, XRD and FTIR results, one could understand the

efficient incorporation of sulphate group in NbOx-DS contributing to higher acidic sites and thus improving the activity.

3.5. TGA analysis

In the case of functionalised solid acid catalysts, the thermal stability of NbOx-D and NbOx-DS is crucial for maintaining the active sites in the catalysts. Thermogravimetric analysis (TGA) is a well-known technique for understanding thermal stability (Figure 6). It was observed that a minor weight loss of 5.1% was observed with NbOx-DS, and a pretty much similar thermograph was obtained for the parent NbOx-D, attributing to the removal of volatile impurities and moisture present in the catalysts. The TGA thermogram of NbOx-DS indicates that the thermal stability of sulfate species is in line with the previous report [54]. Moreover, the thermograph of NbOx-CS (not shown) revealed no significant weight loss due to the absence of sufficient hydroxyl group in niobium oxide lattice, in good agreement with FTIR analysis in which no substantial and intense peak corresponding to OH stretching (2800-3400 cm^{-1}) can be seen. Further, NbOx-DS (113 m^2/g) possessed a 40-fold higher surface area than NbOx-CS (2.9 m^2/g) with negligible pore volume (0.006 cm^3/g) (Table 2), which could be contributing to the enhanced catalytic activity towards the formation of ethyl glucosides.

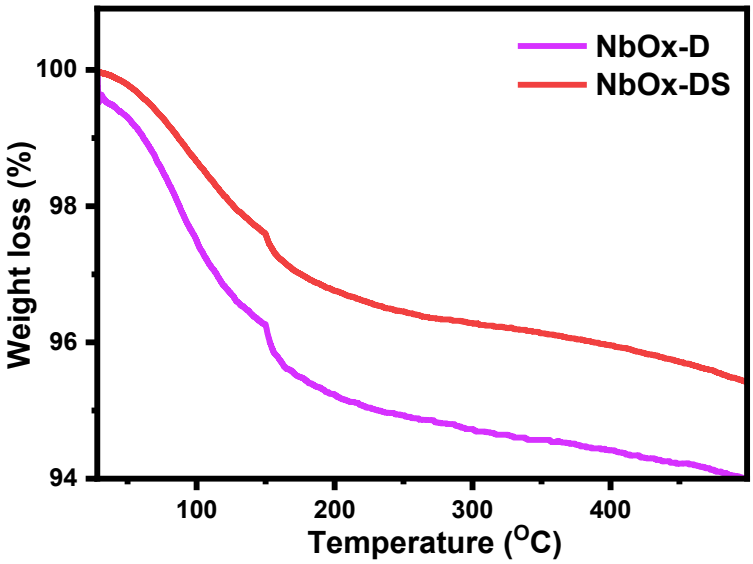

Figure 6. Thermographs of NbOx-D and NbOx-DS catalysts

Table 2. Physicochemical properties of NbOx catalysts

Entry	Catalyst	Surface area (m^2/g)[a]	Pore volume (cm^3/g)[b]	Pore Size (nm)[c]	Type of acidic sites (μmol/g)[d]				
					I	II	III	IV	Total
1	NbOx-D	128	0.208	4.313	137	230	87	174	628
2	NbOx-DS	113	0.164	5.19	47	441	235	60	783
3	NbOx-CS	2.9	0.006	8.38	NA	NA	NA	NA	15

[a]Calculated from BET analysis, [bc]obtained from BJH desorption, [d]calculated from NH_3-TPD analysis.

3.6. Influence of other reaction parameters on yield of ethyl glucopyranosides

The influence of time and temperature on the product distribution was examined, and the results are shown in Figure 7. With an increase in temperature from 80 to 140 °C, the glucose conversion increased from 50 to 80 %, but the yield of ethyl glucosides rose from 16 % (80 °C) to 59 % (120 °C) and then decreased to 22.3% (140 °C), suggesting the formation of humins via degradation of products at higher temperature (Figure 7a). As the reaction time increased from 30 to 240 min, glucose conversion enhanced from 30 to 74%, with an increase in the total yield of ethyl glucosides from 21 to 57.2% (Figure 7b). It was observed that a maximum selectivity (97%) and yield (59%) towards ethyl glucosides were observed at 120 °C with 2 h of reaction time.

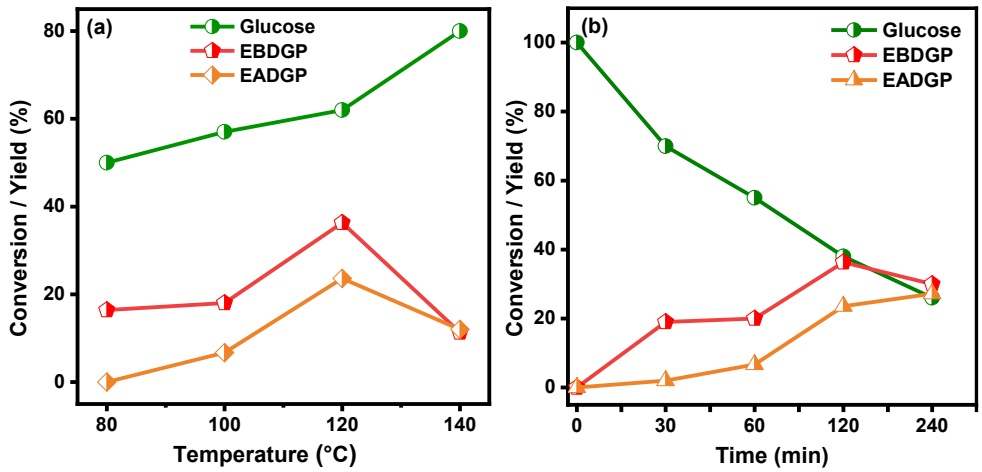

Figure 7. The influence of reaction (a) temperature (Reaction conditions: 0.126 mmol glucose, 20 mg NbOx-DS, 2 h and (b) time (Reaction conditions: 0.126 mmol glucose, 20 mg NbOx-DS, 120 °C).

3.7. Recyclability study

The recyclability of NbOx-DS was also studied in ethanol for three runs, and the results are presented in Figure 8. After each recycle, NbOx-DS was thoroughly washed with ethanol and dried at 100 °C. It was observed that after the first run, there was a slight decrease in glucose conversion and ethyl glucosides yield, suggesting that active species might have been deactivated due to the adsorption of carbonaceous species, thus hindering the accessibility of active sites. However, after the third run, the product distribution was the same as obtained after the second run.

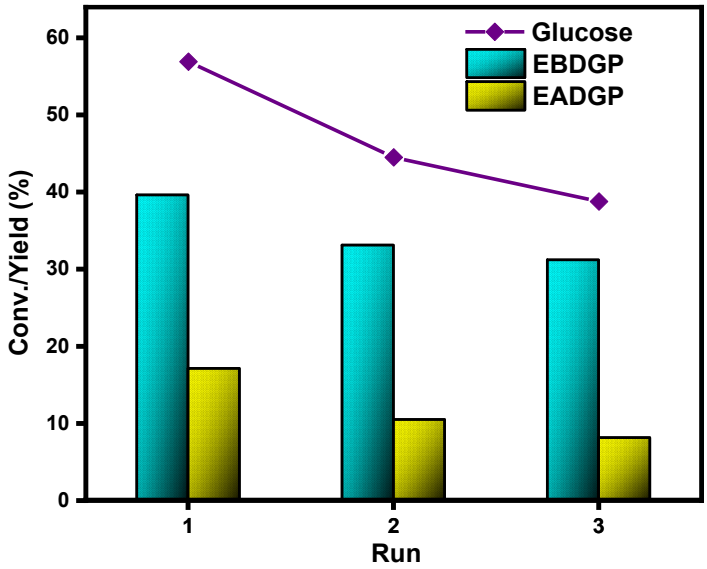

Figure 8. Recyclability of NbOx-DS for acetalation of glucose in ethanol (Reaction conditions: Glucose to catalyst ratio=1.125, ethanol to glucose ratio = 10.1, 120 °C, 2 h.

4. Conclusion

The developed NbOx-D, synthesised via precipitation approach using diethylamine as precipitant, is amorphous in nature and possesses uncondensed hydroxyl groups that pave the way for the efficient incorporation of sulfate species (NbOx-DS), with high thermal stability, achieved through novel NbOx-D synthesis procedure as no such incorporation is achieved with commercial NbOx, due to lack in accessible hydroxyl groups. The NbOx-DS contains 2.1-fold higher acidic sites, thus showing high catalytic activity towards the acetalation of glucose to ethyl glucosides (97% selectivity). In contrast, the previously published article related to glucose acetalation exhibits lower selectivity towards glycosides (<80%) due to the formation

of undesired products and thus deactivating the active sites on the surface of the catalyst. The produced ethyl glucosides have multiple applications in skin care products and cleaning industries. Therefore, the current study signifies further the importance of synthesis of NbOx with defective sites, which facilitates the incorporation of active functional groups, which can be extrapolated to the introduction of auxiliary metals/other functional groups for manoeuvring the strength of acidic sites towards dehydration, esterification and hydrolysis reactions in catalytic industries.

5. Acknowledgment

SK, KS and SS would like to acknowledge the Department of Biotechnology, Government of India, for providing the infrastructural facilities through the Center of Innovative and Applied Bioprocessing for executing the research work. SK and XZ gratefully thank Chemical and Process Engineering, University of Strathclyde, Glasgow, United Kingdom, for allowing access to facilities for performing R&D activities. SK and XZ also thank Civil and Environmental Engineering, University of Strathclyde, for allowing access to HPLC. SK gratefully thank the Newton Bhabha PhD placement program, British Council for fellowship and financial support to carry out this research work and also thankful to Energy Research Centre, Panjab University, Chandigarh, for PhD registration. KS is grateful to the University Grants Commission, New Delhi, India, for providing a Junior Research Fellowship and Indian Institute of Science Education and Research (IISER) Mohali for PhD enrolment.

Declaration of Competing Interest

The authors declare no conflict of interest.

6. References

1. Corma A, Iborra S, Velty A (2007) Chemical Routes for the Transformation of Biomass into Chemicals. Chem.Rev. https://doi.org/10.1021/cr050989d

2. Besson M, Gallezot P, Pinel C (2014) Conversion of Biomass into Chemicals over Metal Catalysts. Chem.Rev. https://doi.org/10.1021/cr4002269

3. Climent MJ, Corma A, Iborra S (2011) Heterogeneous Catalysts for the One-Pot Synthesis of Chemicals and Fine Chemicals. Chem. Rev. https://doi.org/10.1021/cr1002084

4. Lange JP (2015) Renewable Feedstocks: The Problem of Catalyst Deactivation and its Mitigation. Angew. Chem. https://doi.org/10.1002/anie.201503595

5. Lange JP (2016) Catalysis for biorefineries – performance criteria for industrial operation. Catal. Sci. Technol. https://doi.org/10.1039/C6CY00431H

6. Ragauskas AJ, Williams CK, Davison BH, Britovsek G, Cairney J, Eckert CA, Frederick WJ, Hallett JP, Leak DJ, Liotta CL, Mielenz JR, Murphy R, Templer R, Tschaplinski T (2006) The Path Forward for Biofuels and Biomaterials. Science https://doi.org/10.1126/science.1114736

7. Holm MS, Saravanamurugan S, Taarning E (2010) Conversion of Sugars to Lactic Acid Derivatives Using Heterogeneous Zeotype Catalysts. Science https://doi.org/10.1126/science.1183990

8. Aggarwal N, Yatoo MA, Saravanamurugan S (2020) Glucose oxidation to carboxylic products with chemocatalysts. https://doi.org/10.1016/B978-0-444-64307-0.00002-0

9. Kumar S, Devi MM, Kansal SK, Saravanamurugan S (2020) Untangling the active sites in the exposed crystal facet of zirconium oxide for selective hydrogenation of bioaldehydes. Catal. Sci. Technol. https://doi.org/10.1039/D0CY01259A

10. Kumar S, Ali H, Kansal SK, Pandey A, Saravanamurugan, (2020) Sustainable production of sorbitolda potential hexitol. https://doi.org/10.1016/B978-0-444-64307-0.00009-3

11. Kumar S, Kansal SK, Pandey A, Saravanamurugan S (2022) Polyalkylglycosides: sustainable production of nonionic biosurfactants from lignocellulosic biomass. https://doi.org/10.1016/B978-0-12-824419-7.00009-1

12.https://www.icspecialties.com/en/products/surfactants/APG?gclid=CjwKCAjwquWVBhBrEiwAt1KmwsI3PD8e0s8oGyuM0I_YXCoTI9yUTDp4W88c9bn7dm0zhlhmrk9tSBoCrKQQAvD_BwE&gclsrc=aw.ds

13. https://www.nouryon.com/product/ag-6202/

14. https://librachem.co.uk/libra-products-surfactants/libracare-alkyl-polyglucosides/

15.https://www.wanqicn.com/category/alkyl-polyglucoside apg.html?gclid=CjwKCAjwquWVBhBrEiwAt1Kmwn0FzvunN41GpsaOjAViwdlsO7PuKpPwWiteiRJGL2fSnB-WAfhKNxoCwx8QAvD_BwE

16. https://www.galaxysurfactants.com/products/product-groups/mild-surfactants.aspx

17. https://www.biesterfeld.com/en/gb/product/apg/

18. https://librachem.co.uk/libra-speciality-chemicals-hii-cleaning-products/

19.https://www.factmr.com/report/747/alkyl-polyglucoside-market#:~:text=Alkyl%20polyglucoside%20revenues%20were%20up,US%24%201.1%20Bn%20in%202020.

20. Jerome F, Marinkovic S, Estrine B (2018) Transglycosylation: A Key Reaction to Access Alkylpolyglycosides from Lignocellulosic Biomass.ChemSusChem https://doi.org/10.1002/cssc.201800265

21. Wolfgang VR, Karlheinz H (1998) Alkyl polyglycosides - Properties and applications of a new class of surfactants. Angew Chem. 10.1002/(SICI)1521-3773(19980605)37:10<1328::AID-ANIE1328>3.0.CO;2-9

22. Ramdani WG, Karam A, Vigier KDO, Rio S, Ponchel A, Jerome F (2019) Catalytic glycosylation of glucose with alkyl alcohols over sulfonated mesoporous carbons .Mol. Catal. https://doi.org/10.1016/j.mcat.2019.02.016

23. Ma Y, Tan W, Wang K, Wang J, Jiang J, Xu J (2017) An Insight into the Selective Conversion of Bamboo Biomass to Ethyl Glycosides. ACS Sustain Chem Eng https://doi.org/10.1021/acssuschemeng.7b00618

24. Donat R, Demirel V (2022). Synthesis of Some Alkyl Polyglycosides. IJSM. https://doi.org/10.21448/ijsm.1033290

25. Okuhara T (2002) Water-Tolerant Solid Acid Catalysts. Chem Rev https://doi.org/10.1021/cr0103569

26. Harmer MA, Sun Q, Vega AJ, Farneth WE, Heidekum A, Hoelderich WF (1999) Nafion resin–silica nano-composite solid acid catalysts. Green Chem. https://doi.org/10.1039/A907892D

27. Liu F, Huang K, Zheng A, Xiao FS, Dai S (2018) Hydrophobic Solid Acids and Their Catalytic Applications in Green and Sustainable Chemistry. ACS Catal. https://doi.org/10.1021/acscatal.7b03369

28. Wu Y, Yu JG, Ma XF, Zhang JS (2007) An efficient and facile procedure for synthesis of octyl polyglucoside. Chin.Chem.Lett. https://doi.org/10.1016/j.cclet.2007.07.023

29. Puga AV, Corma A (2017) Direct Conversion of Cellulose into Alkyl Glycoside Surfactants. ChemistrySelect. https://doi.org/10.1002/slct.201700389

30. Zheng W, Cui Y, Xu Z, Zhao L, Sun W (2018) Cellulose Transformation into Methyl Glucosides Catalysed by H3PW12O40: Enhancement of Ionic Liquid Pretreatment. Can.J.Chem.Eng. https://doi.org/10.1002/cjce.23057

31. Saravanamurugan S, Riisager A (2011) Solid acid catalysed formation of ethyl levulinate and ethyl glucopyranoside from mono- and disaccharides. Catal.Commun. https://doi.org/10.1016/j.catcom.2011.10.001

32. Siril PF, Davison AD, Randhawa JK, Brown DR (2007) Acid strengths and catalytic activities of sulfonic acid on polymeric and silica supports. J Mol Catal A Chem. https://doi.org/10.1016/j.molcata.2006.11.022

33. Chaugule AA, Jadhav AR, Kim H (2015) Polyvinyl trisulfonate ethylamine based solid acid catalyst for the efficient glycosylation of sugars under solvent free conditions. RSC Adv. https://doi.org/10.1039/C5RA20300G

34. Nakajima K, Baba Y, Noma R, Kitano M, Kondo JN, Hayashi S, Hara M (2011) Nb2O5 3 nH2O as a Heterogeneous Catalyst with Water-Tolerant Lewis Acid Sites. J.Am.Chem.Soc. https://doi.org/10.1021/ja110482r

35. Kitano T, Shishido T, Teramura K, Tanaka T (2013) Characterisation of Thermally Stable Brønsted Acid Sites on Alumina-Supported Niobium Oxide after Calcination at High Temperatures. ChemPhysChem. https://doi.org/10.1002/cphc.201300189

36. Zhou S, Song Y, Zhao J, Zhou X, Chen L (2021) Study on the Mechanism of Water Poisoning Pt-Promoted Sulfated Zirconia Alumina in n-Hexane Isomerisation. Energy Fuels. https://doi.org/10.1021/acs.energyfuels.1c01440

37. Hanaoka T, Takeuchi K, Matsuzaki T, Sugi Y (1990) Niobic acid as a solid acid catalyst for ring-opening reactions of phenyloxirane. Catal. Today. https://doi.org/10.1016/0920-5861(90)87013-S.

38. Heitmann AP, Rocha IC, Periera IM, Oliveira LCA, Patricio PSO (2019) Nanoparticles of niobium oxyhydroxide incorporated in different polymers for photocatalytic degradation of dye. J. Polym. Res. https://doi.org/10.1007/s10965-019-1824-3

39. Wu Z, Li C, Li Z, Feng K, Cai M, Zhang D, Wang S, Chu M, Zhang C, Shen J, Huang Z, Xiao Y, Ozin GA, Zhang X, He L (2021) Niobium and Titanium Carbides (MXenes) as Superior Photothermal Supports for CO2 Photocatalysis. ACS Nano. https://dx.doi.org/10.1021/acsnano.1c00990?ref=pdf

40. Jones BMF, Mamba G, Maruthamani D, Muthuraj V (2022) Honeycomb Nb2O5/RGO wrapped on MoO3 nanorods for visible light-driven degradation of sulfasalazine and ciprofloxacin in water. Colloids Surf. https://doi.org/10.1016/j.colsurfa.2022.129836

41. Rangel EM, Riemke FC, Ucker CL, Raubach CW, Adebayo MA, Machado FM (2022) Photodegradation of acid yellow 23 BY Nb2O5 supported on eco-friendly glass foams. J. Clean. https://doi.org/10.1016/j.jclepro.2022.133231

42. Tagusagawa C, Takagaki A, Iguchi A, Takanabe K, Kondo JN, Ebitani K, Hayashi S, Tatsumi T, Domen K (2010) Highly Active Mesoporous Nb–W Oxide Solid-Acid Catalyst. Angew Chem. https://doi.org/10.1002/anie.200904791

43. Ishikawa S, Shinoda M, Motoki Y, Tsurumi S, Kimura M, Hiyoshi N, Yoshida A, Ueda W (2020) Synthesis of Fluoride-Containing High Dimensionally Structured Nb Oxide and Its Catalytic Performance for Acid Reactions. Inorg. Chem. https://doi.org/10.1021/acs.inorgchem.0c00949

44. Yamashita K, Hirano M, Okumura K, Niwa M (2006) Activity and acidity of Nb2O5-MoO3 and Nb2O5-WO3 in the Friedel-Crafts alkylation. Catal. Today https://doi.org/10.1016/j.cattod.2006.07.025

45. Hegde V, Pandit P, Rananaware P, Brahmkhatri VP (2021) Sulfonic acid-functionalised mesoporous silica catalyst with different morphology for biodiesel production. Front Chem Sci Eng https://doi.org/10.1007/s11705-021-2133-z

46. Testa ML, Parola VL (2021) Sulfonic Acid-Functionalized Inorganic Materials as Efficient Catalysts in Various Applications: A Minireview. Catalysts https://doi.org/10.3390/catal11101143

47. Sturt NRM, Vieira SS, Moura FCC (2019) Catalytic activity of sulfated niobium oxide for oleic acid esterification J. Environ. Chem. Eng. https://doi.org/10.1016/j.jece.2018.102866

48. Ngee ELS, Gao Y, Chen X, Lee TM, Hu Z, Zhao D, Yan N (2014) Sulfated Mesoporous Niobium Oxide Catalysed 5-Hydroxymethylfurfural Formation from Sugars. Ind. Eng. Chem. Res. https://doi.org/10.1021/ie501980t

49. Rathnayake D, Perera I, Amin AS, Kerns P, Dissanayake S, Suib SL (2020) Mesoporous Crystalline Niobium Oxide with a High Surface Area: A Solid Acid Catalyst for Alkyne Hydration. ACS Appl. Mater. Interfaces. https://doi.org/10.1021/acsami.0c10757

50. Goetze J, Yarulina I, Gascon J, Kapteijn F, Weckhuysen BM (2018) Revealing Lattice Expansion of Small-Pore Zeolite Catalysts during the Methanol-to-Olefins Process Using Combined Operando X-ray Diffraction and UV−vis Spectroscopy. ACS Catal. https://doi.org/10.1021/acscatal.7b04129

51. Selvaraj M, Venktachalapathy V, Mayandi J, Karazhanov S, Pearce JM (2015) Preparation of meta-stable phases of barium titanate by Sol-hydrothermal method. AIP Adv. https://doi.org/10.1063/1.4935645

52. Li N, Wang A, Liu Z, Wang X, Zheng M, Huang Y, Zhang T (2006) On the catalytic nature of Mn/sulfated zirconia for selective reduction of NO with methane. Appl. Catal.B https://doi.org/10.1016/j.apcatb.2005.08.007

53. Wang Q, Jiang H, Gong H, Chu G, Lin C, Dong X (2012) Synthesis, characterisation and thermal stability of a crystalline niobium oxysulfate. J. Alloys. Compd. https://doi.org/10.1016/j.jallcom.2012.01.033

54. Gheit AKA, Desouki DHE, Hamid SMA, Ghoneim SA, Ibrahim GH, Gad FK (2012) Sulfated Zirconia Catalysts for Low Temperature Isomerisation of n-Pentane. Egypt. J. Chem. https://dx.doi.org/10.21608/ejchem.2012.1171

55. Jerome F, Marinkovic S, Estrine B (2018) Transglycosylation: A Key Reaction to Access Alkylpolyglycosides from Lignocellulosic Biomass ChemSusChem https://doi.org/10.1002/cssc.201800265

56. Li X, Peng K, Liu X, Xia Q, Wang Y (2016) Comprehensive Understanding of the Role of Brønsted and Lewis Acid Sites in Glucose Conversion into 5-Hydromethylfurfural. ChemCatChem https://doi.org/10.1002/cctc.201601203